Journal homepage www.jzs.univsul.edu.iq
Journal of Zankoy Sulaimani
Part-A- (Pure and Applied Sciences)

Extraction and Analysis of Tectonic Lineaments using Geoinformatic Techniques, in Tawke Oil Field, Duhok area, Iraqi Kurdistan Region

Abdulla Amir Omar[1]& Rebar Tahssen Ali[1]

[1] University of Salahaddin-College of Science- Department of Geology- Iraq-Kurdistan region-Arbil
Abdulla.omar@su.edu.krd

Article info

Original: 06.10.2015
Accepted:13.04.2016
Published online:
01.05.2016

Key Words:
Satellite-images, Lineaments, seismic, gravity, fractures.

Abstract

Geoinformatic techniques applied for tectonic lineament extraction and analysis in Tawke Oil field, Kurdistan region of Iraq. Two satellite images have been used, which were Landsat ETM+ and ASTER images to extract lineaments both visually and automatically. It comprises several steps, which involve several enhancing techniques e.g. Color Composite, Spectral Rationing and Principle Component Analysis. From combination of all techniques, the final surface lineaments have been extracted. The final lineament map has been divided in to two maps; local lineament map which was checked in the field and regional lineament map which was confirmed by geophysical data (seismic and gravity data). Local lineaments are evaluated in order to extract further information on the spatial distribution and nature of the lineaments. For this purpose lineament density, length, and lineaments intersection maps are prepared. In addition; the field work was carried out to verify lineaments resulted from satellite images with the observed fractures on the ground through visiting of 17 stations around the Tawke anticline. Orientations of local lineaments (frequency and length) obtained from satellite image were compared with the orientation of fractures (frequency and length) that obtained from the field, using rose diagrams which show a similarities between them, as being concentrated in NE-SW, NW-SE, E-W and N-S, as well as these Lineaments reflect a set and systems of fractures with in studied outcrops. Two types of fractures are recognized one are shear fractures and second are tension fractures. Stereographic projection figured out for confirming the direction of fractures in the field and analyzing the paleostress direction within studied area.

Geophysical data (gravity and seismic) have been used for confirming the regional lineaments. Integration has been made between satellite image lineaments and lineaments appeared in geophysical data (gravimetric and seismic lineaments) , there is a coincidence both in the positions, length and azimuths of gravimetric lineaments, seismic lineaments and lineaments appear on satellite image (i.e. surface lineaments). It has been observed that two mechanisms are responsible for giving the architectural shape of study area one is due to block-faulting related to basement faults activity from at least the Middle Paleozoic and continued intermittently up to Late Tertiary, while the second mechanism is due to compressive horizontal stress that have been active since Middle – Late Cretaceous continued up to Late Tertiary.

1. Introduction

The use of new technologies in geology has been promoted for a while, especially the geo-informatics technology (i.e. remote sensing (RS), Geographic Information Systems (GIS) and Global positioning System (GPS)) applications which are called (3S technology). Geoinformatic percolates into common life since the utility of these technologies has a variety of uses in multidiscipline such as Geology, Environmental Sciences, land information system and engineering, agriculture…etc. Geoinformatic technique has been used effectively for geological applications. For example, mapping of lineaments or structural linear features of any region may provide useful information for tectonic and mineral or oil exploration studies ***[1,2,3,4]***. Lineament analysis techniques using remotely sensed data help researchers to identify different structural regimes and tectonic zones. Lineaments are significant lines that reveal the hidden architecture of the landscape that reveal the hidden architecture of the rock basement. However lineament define as a mappable, simple or composite linear feature of a surface whose parts are aligned in a rectilinear or slightly curvilinear relationship and which differ from the pattern of adjacent features and presumably reflects some sub-surface phenomenon ***[3]***. Remotely sensed lineaments are often used as indicators of major features in near surface. Earlier, lineament interpretations were made from aerial photographs. Recently, geologists have been interested in tracing lineaments from satellite images which have broad coverage under the uniform conditions.

2. Study area:

The studied area is Tawke Oil field within Tawke anticlinal Structure in the city of Zakho - Duhok governorate, northern Iraq, the area range in elevations between 350m to1600 m above sea level and the study area covers about 645 km^2 (Figure- 1). The Tawke Oil field is located in the high folded zone of Zagros- Taurus Folds and Thrust belt. It is one of the largest oil field in Iraqi Kurdistan Region and produces high-gravity oil from fractured reservoir at depth of 1 km. Norwegian oil and Gas Company; DNO redeveloped the field from 2004 and commenced production in June 2007. The Tawke export infrastructure was connected with the Iraq-Turkey pipeline system early 2009 to deliver crude oil to the international market. The original level of production averaging 50,000 b/d of oil was increased to a proved sustainable production capacity of nearly 70,000 b/d in 2011 and raised up to 100,000 b/d in 2012. In March 2012, a revised, independent estimate of more than 700 million barrels was confirmed at Tawke, proving that Tawke is a world-class giant oil field. According to the strategy of the company the capacity of oil will reach to 200,000 – 400,000 b/d in 2015to 2016 ***[5].***

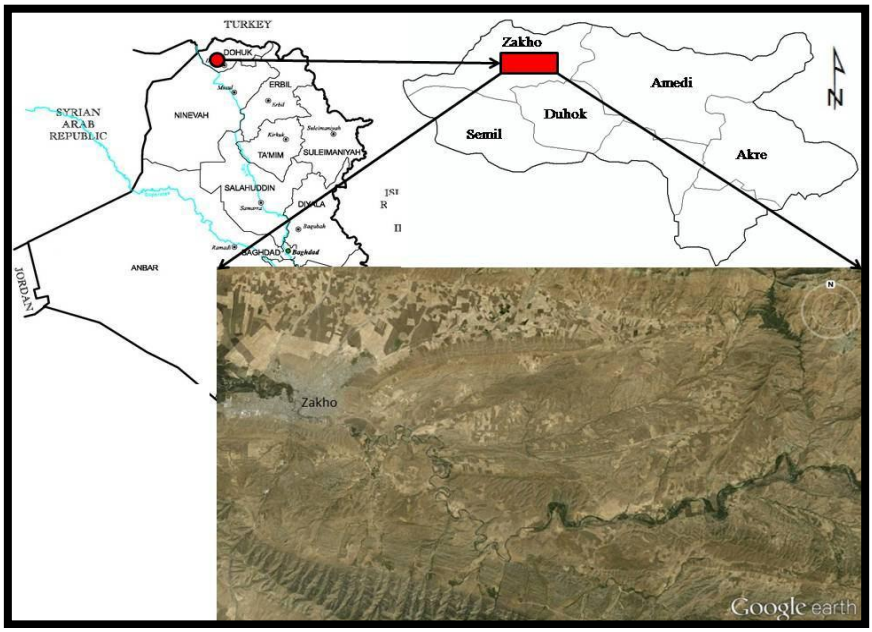

Figure-1: The location map of the study area.

3. Material used and Methodology:

The origin and tectonic analysis of lineaments needs using of different data sets and material for that three level of obtaining data are used (Figure 2), one level of data are from remote sensing data(Satellite images), the second level of data are obtained from field ground truth, while the third level are from geophysical data (Seismic and Gravity data). Data acquisition from products of Remote sensing devices was carried out in the office from Landsat ETM+ image and ASTER image. Different Software's were used for image processing, extracting of lineaments and statistical analysis as well as presentation of the maps, such as ENVI 4.5, Geomatica 9.1 and Arc Map 10. Field data are represented by fractures and bedding planes also analyzed using stereographic projection techniques. Geophysical data (seismic, gravity) was also used for confirming the Regional lineaments within studied area. The seismic data received from Ministry of Natural Resources, KRG while gravity data obtained from previous studies.

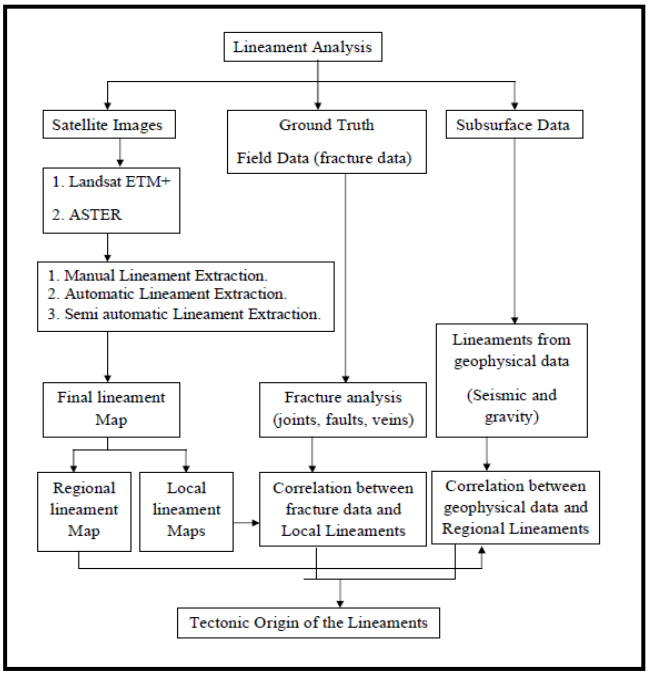

Figure-2: Flowchart showing the different stages applied in this study.

4. Geologic Setting

4.1. Structural style of the studied area:

The Tawke anticlinal structure is located within Zagros-Taurus Fold and Thrust belt in northern segment of Iraqi territories. Tectonically this structure located between two different Iraqi tectonic zones, which are low folded zone to the south and imbricated zone to the north. The topography of the area was obviously reflecting structural features. The presence of folds, faults and major fractures has significant role either in shaping or given complexity to the area (Figure-3). Pi-diagram which revealing one field cross section passing through middle part of the structure (Figure-4) show that this structure is asymmetrical, cylindrical, double plunging anticlinal fold , with fold axis attitude 094/04. The stereographic projection indicates that the attitude of northern limb and southern limb are 007/38, 175/25 respectively, this indicates that the vergency of this anticline is toward the north, which is abnormal case with respect to other folded structures in this region. The interlimb angle as measured from stereographic projection (Figure -4) is 114 degree so it's classified as open, horizontal up-right fold, as well as the constant orthogonal thickness of folded beds throughout all parts of this fold indicates that this fold is Class 1B type. The presence of slickensides along most of the bedding planes is a good indicator for mechanism of flexural-slip folding type

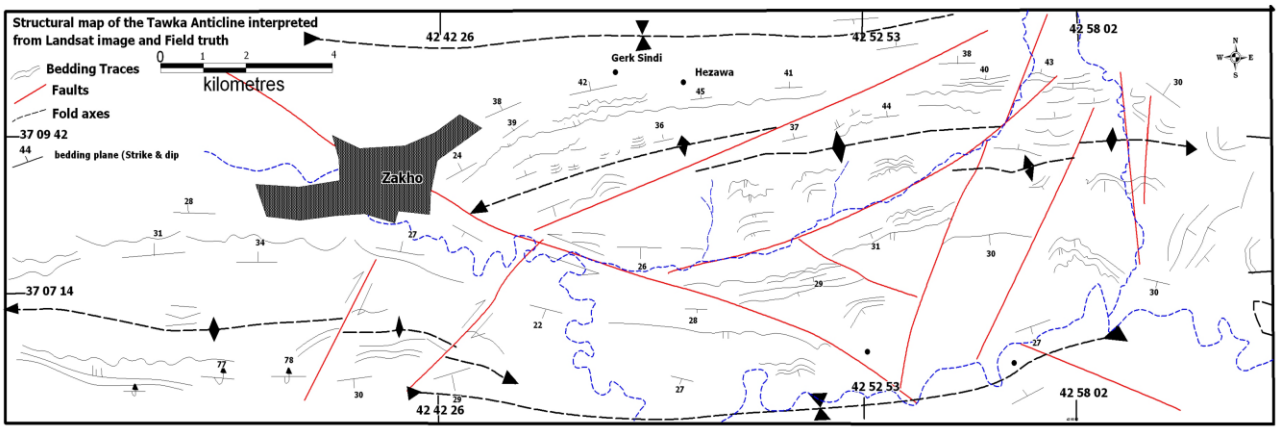

Figure -3: Structural map interpreted from Landsat ETM+ image & field measurements for Tawke structure.

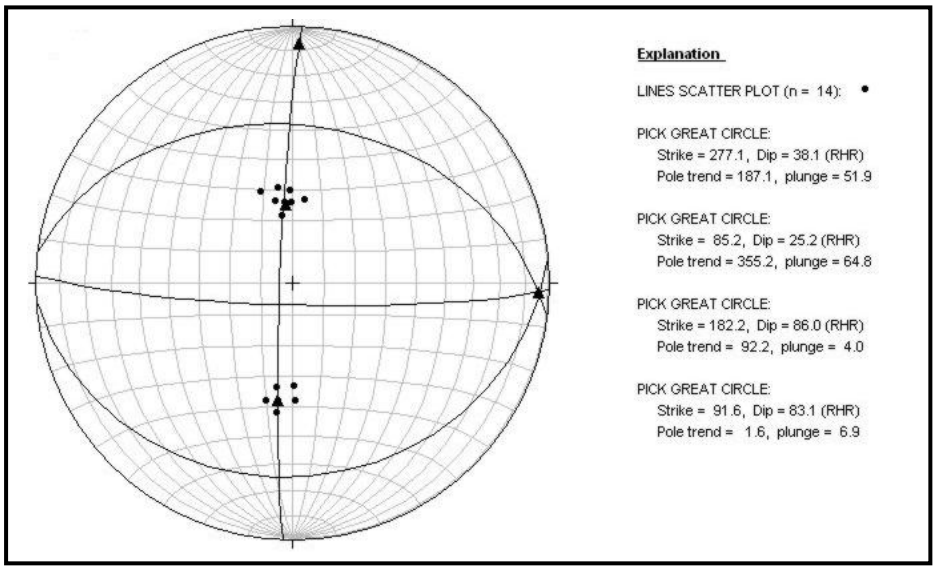

Figure-4: The pi-diagram of bedding planes with geometrical properties of the Tawke anticlinal structure across central part.

A number of major faults struck this structure in different directions, mostly in NNE-SSW, NE-SW and NW-SE trends (Figure-3), these faults are either strike slip types or reverse (Thrust) type, the faults causes displacements in outcrops of bedding plane traces, as well as cause displacing the fold axis in different parts of the structure, the displacing range between 100-450m either sinisterly or dextrally. Due to these displacements in fold axis this structure appears as complicated type especially at western plunge area with high number of faults cross cutting this part. Most of these major faults reflect deep seated subsurface faults which later propagated upwards to surface (Later will be discussed).

4.2. Stratigraphy:

The Tertiary rock units of Iraq comprise many economically important units particularly in Oligocene and Miocene ***[6].*** The stratigraphic formations that observed in studied area from older to younger are Gercus Formation (Middle Eocene), Pila Spi Formation (Middle-Late Eocene), Fatha (Lower Fars) Formation (Middle Miocene), Injana (Upper Fars) Formation (Late Miocene), Mukdadyah (Lower Bakhteari) Formation (Lower Pliocene), Bai Hassan (Upper Bakhteari) Formation (Pliocene), and Quaternary sediments. The distribution of the Formations within the studied area is shown in (Figure-5). A generalized stratigraphic column of succession is also constructed for showing lithological properties of the formation in the studied area (Figure- 6).

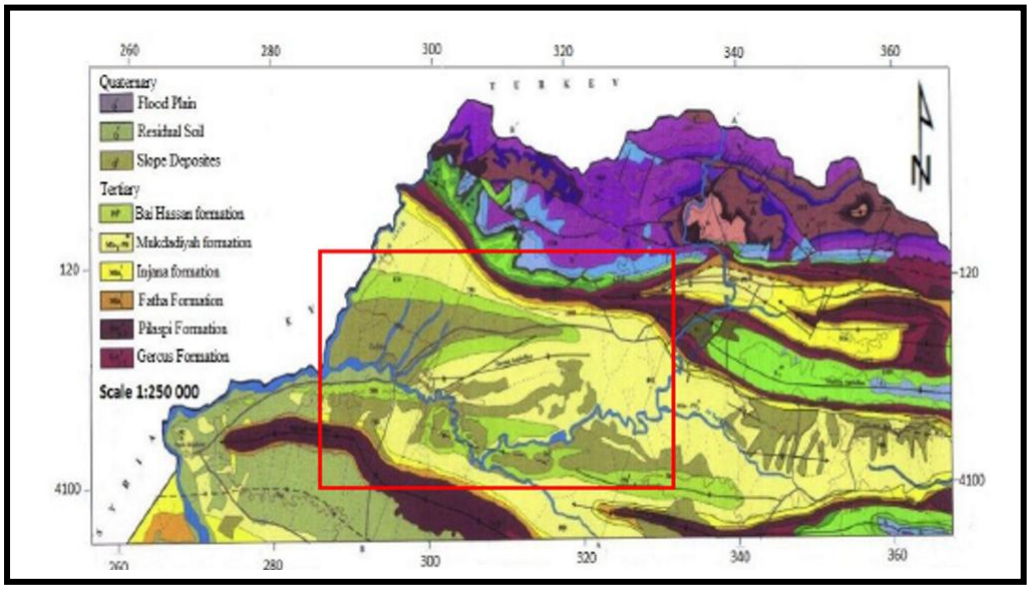

Figure-5: Geological map of the studied area *[7].*

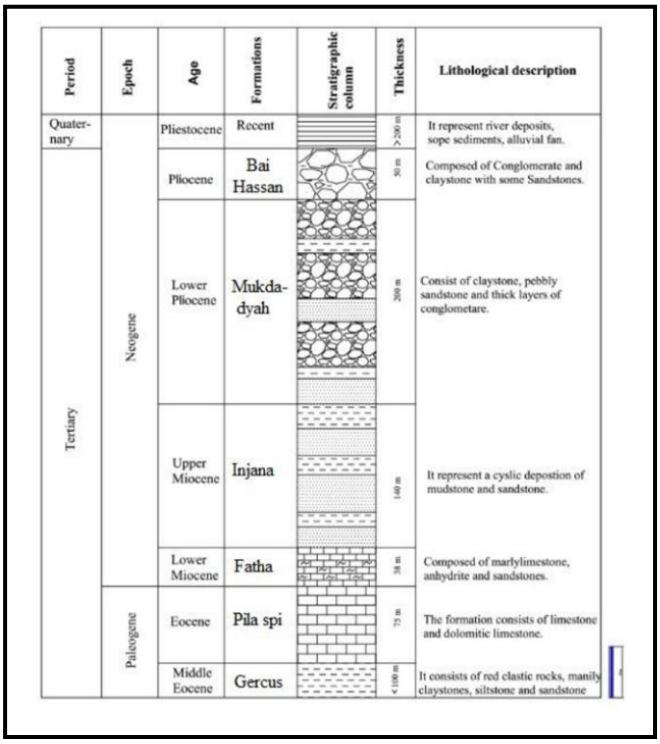

Figure-6: Stratigraphic column of the studied area *[7].*

5- Extraction and analysis of lineaments:

Different remote sensing techniques for lineament extraction are used which are:

5.1. Lineament Extraction from Satellite Imagery:

Lineament extraction and analysis is one of the routines in mapping large areas using remotely-sensed data, most of which is the satellite images. In this study, we used both Landsat ETM+ and ASTER images to test and evaluate the differences lineament extraction techniques.

5.1.1. Manually lineament extraction from Landsat ETM+images:

In manually extraction method, the lineaments were extracted from satellite image using visual interpretation. Different criteria were used in order to delineate these lineaments, such as straight valleys, continuous scarps, tonal variations, straight segment of stream or rivers, rock boundaries, sudden deflection in river or drainage directions and alignment of vegetation along a line ***[8, 9, and 10]***.

Preparing convenient Landsat images for manually lineament interpretation are necessary first , so for that several image enhancement techniques are used ***[11,12]*** . In this study three of commonly known techniques have been used in the preparation of the final lineament map. These are color composites (Figure:7a), spectral rationing (Figure:7b),and Principal Component Analysis (PCA) (Figure:7c). The main reason for using several techniques is that one single method may not detect all the lineaments because of the variation in the nature of surface material in the area such as variations in the vegetation density, topographic texture and elevation.

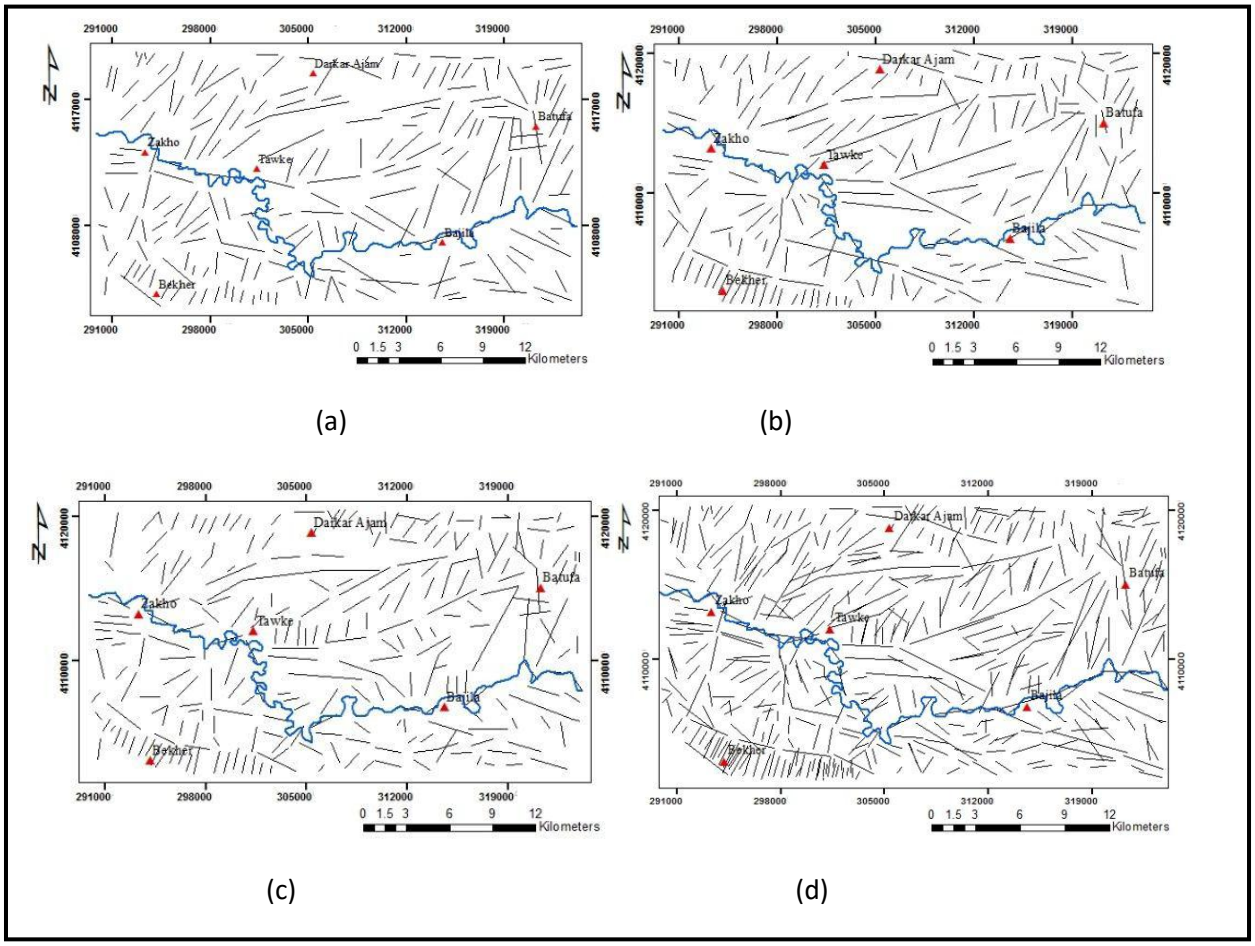

Figure-7: a): Lineaments extracted from color composite of the band 7 (Red), 4 (Green), 2 (Blue).
b): Lineament map extracted from band rationing. C): Lineaments extracted from PCA d): Final lineament map generated by the combination of different methods (a,b,c).

Single lineament map (Figure -7d) was generated from these three maps (Figures-7a,b,c) in which the repeated lineaments were deleted. Duplicated lineaments in the three stages give high confidence to the final lineament map. Total number of lineaments generated by different methods was 665. The total number in the final map is 513, suggests that 152 lineaments were deleted that not corresponding to actual lineaments due to low degree of confidence .The percentage of lineament confidence in all three manually extracted methods (color composite, spectral rationing and PCA) equal to 77.2%.

5.1.2. Automated Lineament Extraction from ETM+:

Lineaments are extracted from satellite images using automated extraction techniques in order to compare with the manually extracted lineaments. The main advantages of automated lineament extraction over the manual lineament extraction are its ability to uniform approach to different images; processing operations are performed in a short time and its ability to extract lineaments which are not recognized by the human eyes.

firstly; ENVI 4.5 software has been used for extracting lineament automatically by using Directional Gradient-Sobel filter to the Landsat ETM+ band 7 in N-S, E-W, NE-SW and NW-SE directions to increase frequency and contrast in the image***[13,14]***. The directional filters in four principal directions are given in (Table- 1).

Table -1: Sobel filter in four main directions applied in this study.

	N-S			NE-SW			E-W			NW-SE		
Sobel	-1	0	1	-2	-1	0	-1	-2	-1	0	1	2
	-2	0	2	-1	0	1	0	0	0	-1	0	1
	-1	0	1	0	1	2	1	2	1	-2	-1	0

Secondly; the PCI Geomatica software has been used which provides different algorithms for automated extraction. LINE module of Geomatica extracts linear features from an image and records the polylines in vector segments by using six parameters, RADI=12 GTHR=40 LTHR=15 FTHR=2 ATHR=30 DTHR=1.The results of the Sobel filter is given in (Figures 8 ,9,10 and 11) for four main directions. The number and percentage of Lineaments extracted from each direction is given in (Table-2). Furthermore, histogram and basic statistics for each dominant direction are carried out as a result a maximum number of Lineaments detected in E-W direction and a minimum number of Lineaments recorded in N-S direction.

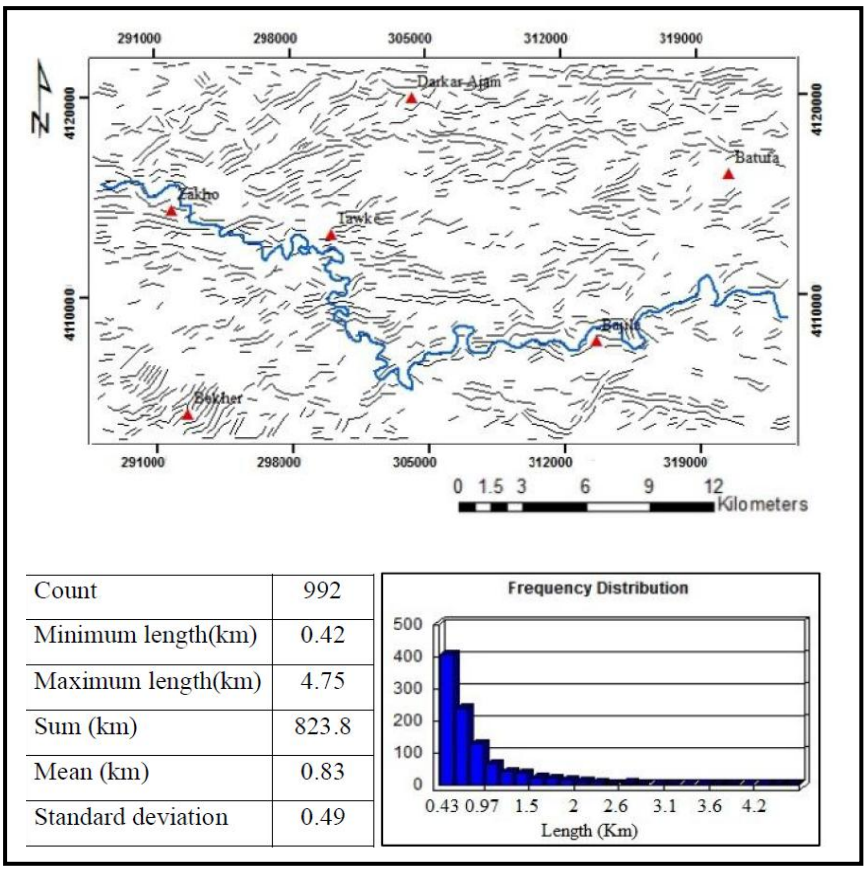

Figure-8: Lineament map of E-W directions with statistical analysis using Sobel filter.

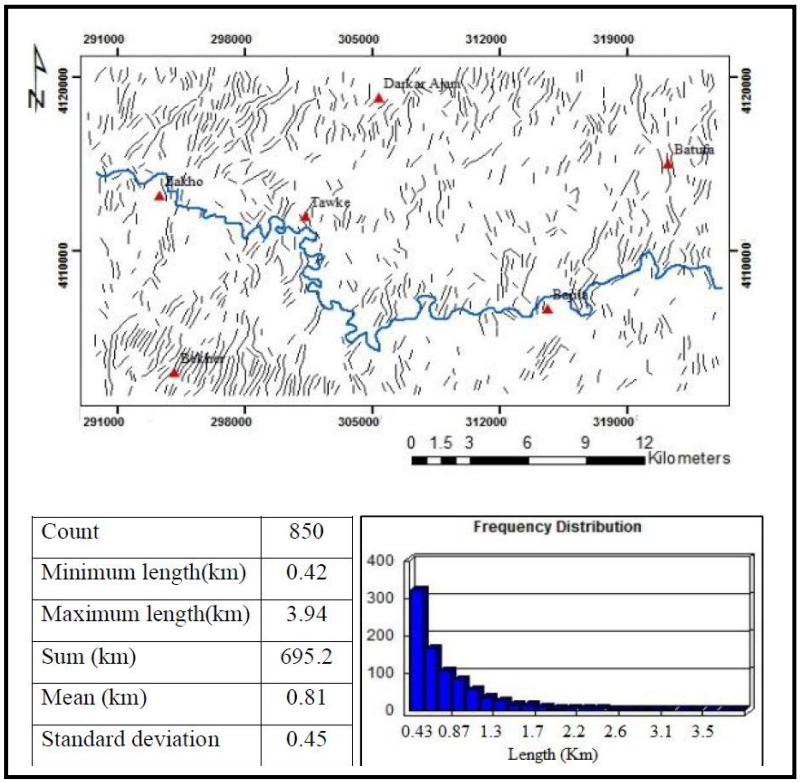

Count	850
Minimum length(km)	0.42
Maximum length(km)	3.94
Sum (km)	695.2
Mean (km)	0.81
Standard deviation	0.45

Figure-9: Lineament map of N-S directions with statistical analysis using Sobel filter.

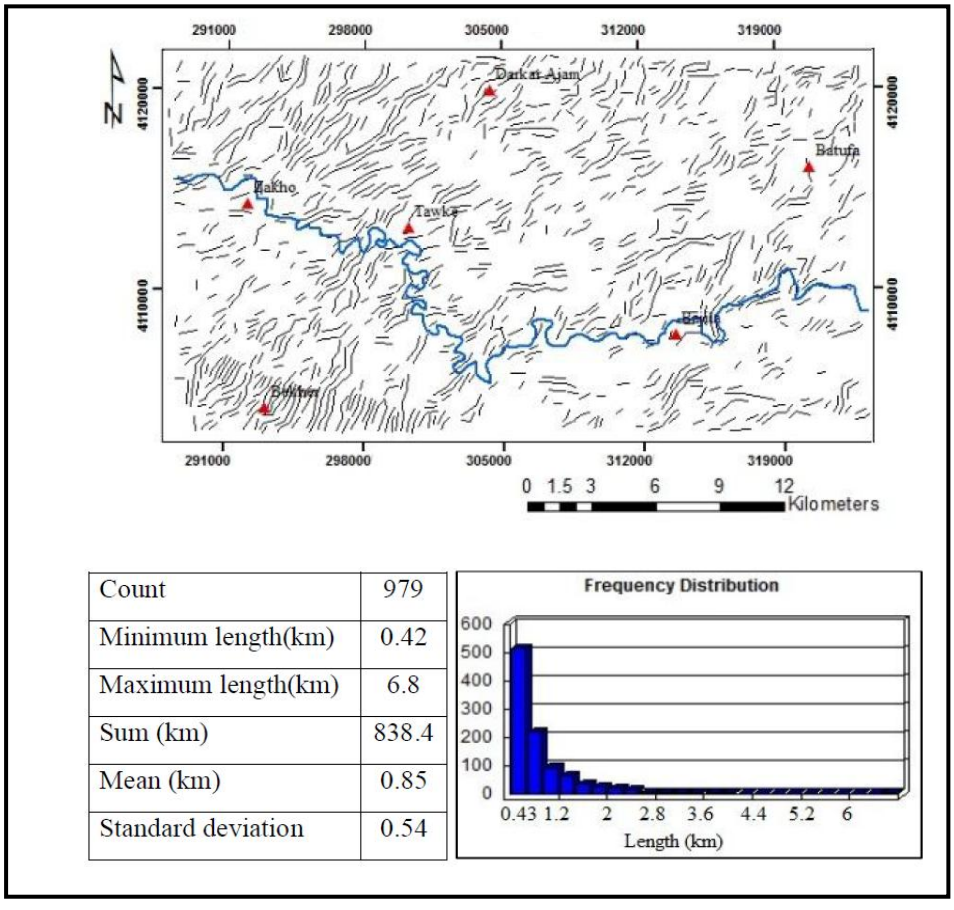

Count	979
Minimum length(km)	0.42
Maximum length(km)	6.8
Sum (km)	838.4
Mean (km)	0.85
Standard deviation	0.54

Figure-10: Lineament map of NE-SW direction with statistical analysis using Sobel filter.

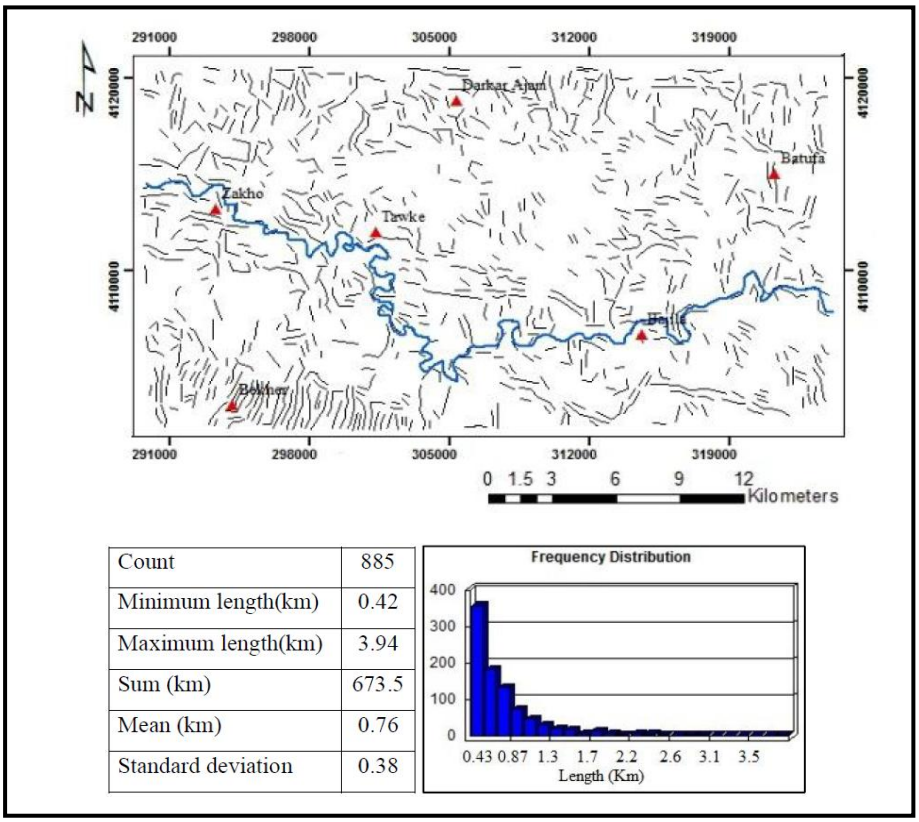

Figure-11: Lineament map of NW-SE direction with statistical analysis using Sobel filter.

Table -2: The number and percentage of Lineaments extracted from each directions.

Sr.	Direction	No. of Lineaments	% of lineaments
1	N-S	850	22.9 %
2	E-W	992	26.8 %
3	NE-SW	979	26.4 %
4	NW-SE	885	23.9 %
Total		3706	100 %

5.1.3. Manually lineament extraction from ASTER images:

Delineation of lineaments manually from ASTER image was performed by selection of optimum band combination to obtain visually maximum possible color contrast. During this process, several band combinations were examined in order to enhance the images for discriminating the geologically meaningful linear features from the artifacts. Among various band combinations, the combination of bands 321in RGB respectively found to be the combination having the best spatial resolution ***[15]*** (Figure-12a). As a result 235 lineaments were extracted (Figure-12b).

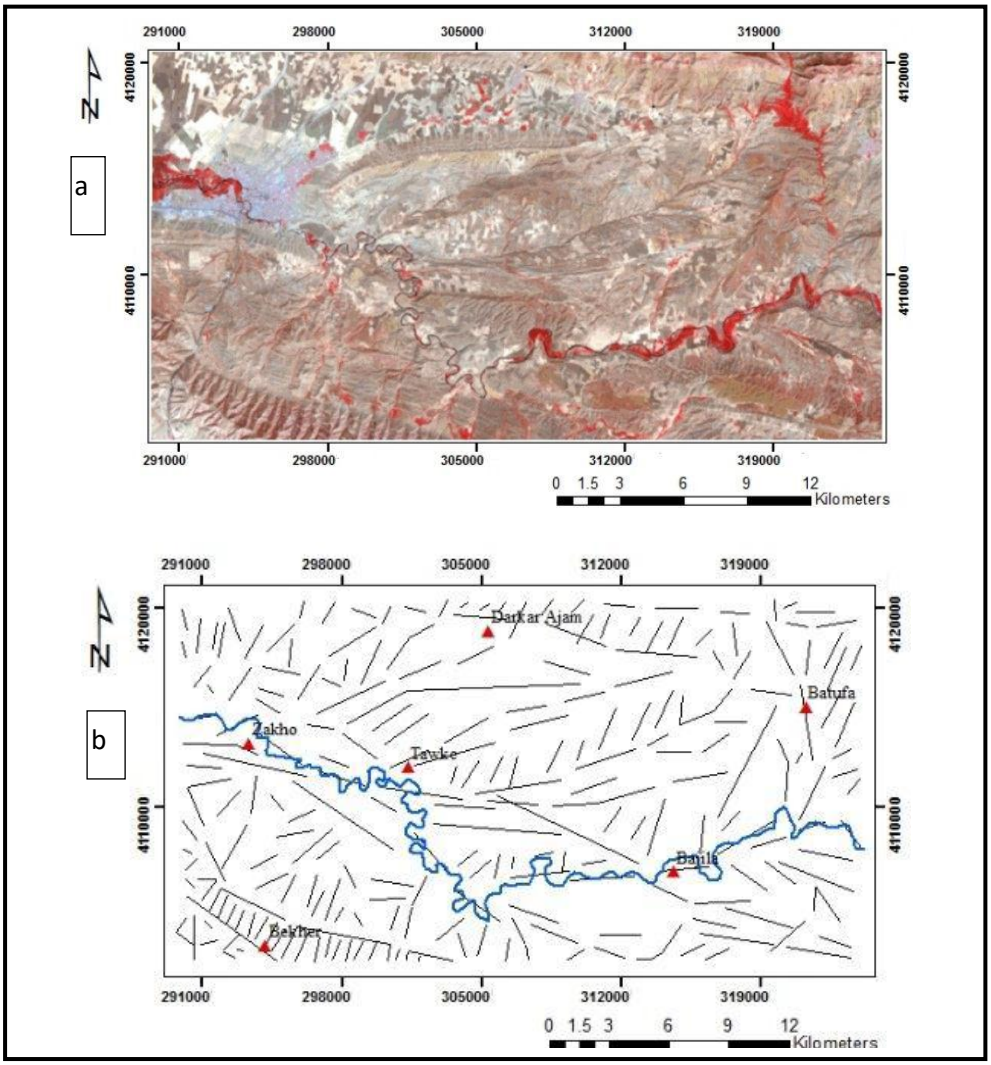

Figure -12: a): color composite image of the band 3 (Red), 2 (Green), 1 (Blue) for ASTER image. b): Lineament map extracted from color composite of RGB 321 of Aster image.

5.1.4. Automatic Lineament Extraction from ASTER images:

The Automatic lineament extraction process for ASTER data was also carried out with LINE module of PCI Geomatica and same procedures that are performed on the Landsat data were applied but different parameters have been selected. Due to constraints explained in Landsat ETM+ section, the band 3 was selected as an input channel for LINE algorithm it is thought that the band 3 is the best choice due to having longer wavelength. Therefore, it gives good contrast and display geological lineaments compared to other bands because the contrast loss due to atmospheric haze is minimal ***[16]***. The parameters in this application were selected as: RADI=1 GTHR=30 LTHR=50 FTHR=3 ATHR=15 DTHR=150. By using these parameters 777 lineaments were extracted as seen in (Figure-13).

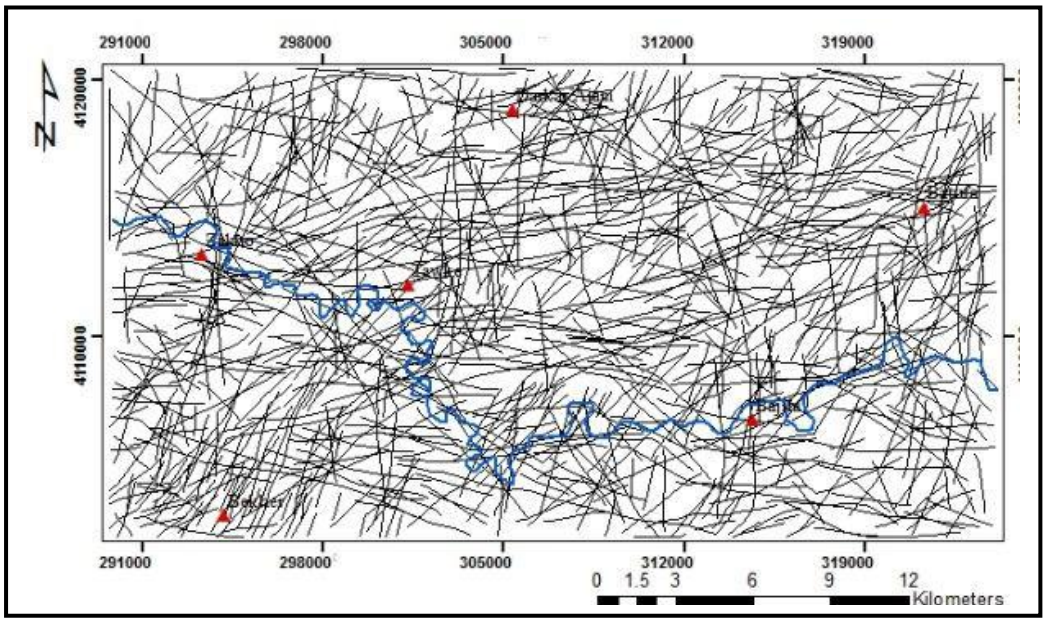

Figure-13: Automatically Extracted Lineaments from Aster image.

5.2. Final lineaments Map (Combination of two lineament Maps):

The previous mentioned techniques and steps were used to extract the Lineaments from both satellite images Landsat ETM+ and ASTER. These two Lineament maps were combined together to generate one map using a GIS technique (Figure-14). The reason for selecting one final lineament map instead of multiple Lineament maps may result in confusion and complexity when comparing to other geological data. From combining both maps a number of 2417 Lineaments were extracted. The total number in the final map are 1519, suggests that 862 Lineaments were deleted because they are not corresponding to Lineaments of structural origin and it is believed that these Lineaments belongs to non-geological Lineaments such as roads, fences, field boundaries and farmland area. This number was carried out from manually methods and field checking and it gives low degree of confidence as it is seen in Figure-14. The percentage of Lineament confidence from combining both satellite images equal to 78%. Total length of all Lineaments equal to 2130.4 km. Length of maximum Lineament detected is 12.41 km, however, is 0.37 km for the minimum length (Table-3).

Orientations of Lineaments are compared using frequency and length of Lineaments (Figure14). In frequency rose diagram the maximum number of Lineaments are trending in 095◦ direction which is classified as first order trend, another set of Lineament trending 065◦ which classified as a maximum second order, while the third maximum order of Lineament oriented toward 075◦. Minimum number of Lineaments recorded in a direction of 150◦ (first order) while minimum second order and third order are in directions of 165◦ and 185◦ respectively. In length rose diagram the maximum first order has the same direction of maximum first order in frequency which is 095◦. It is a good indicator that the majority of Lineaments have EW direction and it confirms to Taurus Mountain in Turkey. Maximum second order trending 075◦, while maximum third order contains the two subordinate directions of Lineaments that can be seen in 015◦ and 025◦. Also minimum number of Lineaments oriented as 145◦ which is classified as first order, while minimum second and third order of Lineaments are trending 165◦ and 155◦ respectively (Table-3).

Rose diagram of the Lineaments (i.e. frequency and length) shows two set of tension fractures which are frequently associated with trend of the Tawke structure trending EW and N-S direction. Also two set of shear fractures coincides with regional fractures that trending NW-SE and NE-SW.

Table-3: Orders of frequency and length lineament directions within study area.

	Frequency		Length	
Orders	Maximum	Minimum	Maximum	Minimum
First order	095°-275°	150°-330°	095°-275°	145°-325°
Second order	065°-245°	165°-345°	075°-255°	165°-345°
Third order	075°-255°	185°-355°	015°-195°	155°-335°

5.3. Analysis and Spatial distributions of tectonic Lineaments:

Length-frequency histogram (Figure-14b) indicate that the majority of lineaments appears in two groups of length, so they classified into two types, namely regional (length >5km) and local (length < 5km). The number of short lineament type are 1510 lineaments, which is equal to about 98.3% of the existing lineaments, while there are nine lineaments which are equal to 1.7%, and classified as regional lineament type.

5.3.1. Regional Lineaments Analysis:

The study area consist nine regional lineaments cross the study area (Figure15) and are extend for several kilometers in length, they trend almost in all direction but northeastern direction is most predominant than the other directions and appears to effect the structural architecture of the studied area. The most characteristic properties of these lineaments are showing in Table-4.

Some of these lineaments are documented by Iraqi oil Exploration company, such as Lineament 4and,5 or other lineament such as lineament 7 documented by***[17,18,19]*** . The resets of lineaments not recognized by any one and they are delineated for the first time in this study. Some of these regional lineaments appears as a strike slip faults in characteristic causing displacement either in outcrops of the beds or displacing Tawke fold axis as in the case of lineaments 4,5,6,7 which giving rise to complex shape of this structure.

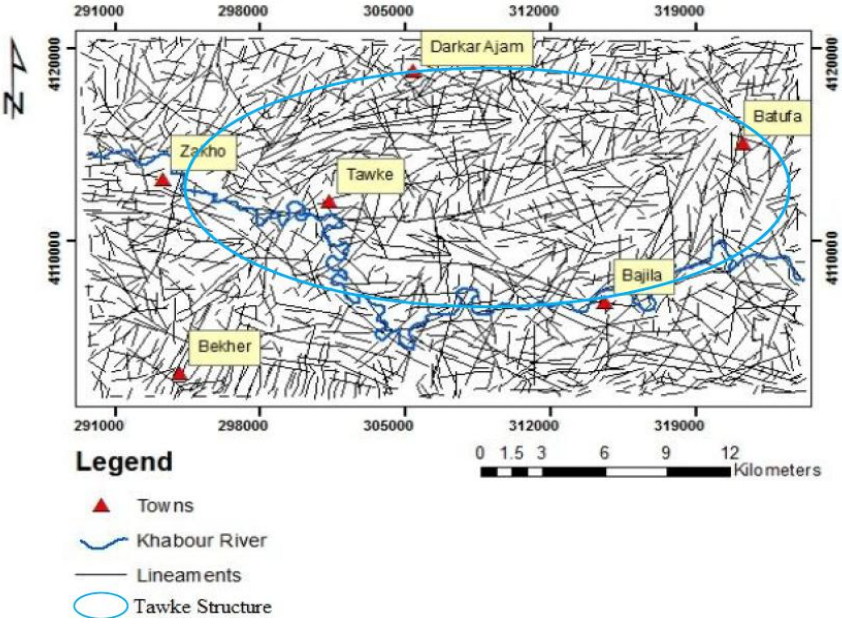

(a)

Count	1537
Minimum length (km)	0.37
Maximum length (km)	12.4
Sum (km)	2130.4
Mean (km)	1.38
Standard Deviation	1.18

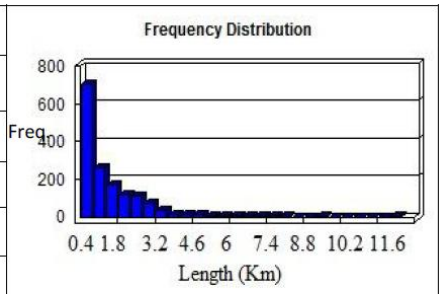

(b)

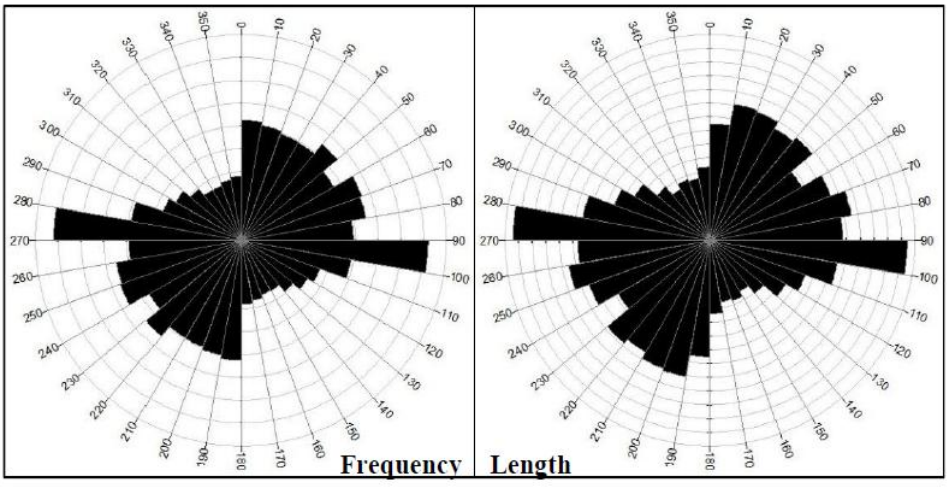

(c)

Figure -14: Final Lineament map (a) with its statistical analysis (b) frequency and length rose diagram (c) for lineaments.

Table-4: Most characteristic properties of regional lineaments within studied area

Lineament numbers	*Main Direction*	*Length in Km*	*Remarks*
1	*N 30 E*	*15.5*	*Cause deflection in Khabour river*
2	*N 35 E*	*6.87*	*Cause deflection in Khabour river*
3	*N 75 W*	*24.19*	*Coincide with Khabour river*
4	*N 73 E*	*18.34*	*Cause displacement in out crops*
5	*N 85 E* *N 60 E*	*23.7*	*Curvilinear Lineament* *Cause displacement in out crops*
6	*N 25 E*	*17.29*	*Cut and complicate the eastern plunge of Tawke structure*
7	*N 24 E*	*17.32*	*Cut eastern plunge of Tawke structure, give complicated form of structure*
8	*N 15 W*	*8.81*	*Displaced Tawke fold axis*
9	*N 72 W*	*8.15*	*Cause deflection in Khabour river*

5.3.2. Geophysical Confirmation of Regional Lineaments:

Potential field; gravity, seismic reflection profiles and remote sensing data provide important direct or indirect information on basement depth, structure, tectonics and composition. Integration has been made between Lineaments obtained from satellite image and Lineaments appeared in geophysical data (gravimetric and seismic Lineaments) by displaying the GIS layer of regional lineaments with the Lineaments that have been detected from geophysical data. A new map was obtained which is shown in (figure-16). In present study, there was an appreciable similarity both in the positions, azimuths and length of gravimetric Lineaments, seismic Lineaments and regional lineaments appear on satellite image (i.e. surface Lineaments).Some of subsurface faults propagated upwards through thick depositional panel, and sometimes due to difference in competency between different layers the faults at the surface shifted away from exact place of original position ***[20]***.

5.3.2. Local Lineaments Analysis:

The largest numbers of extracted lineaments in the studied area are local lineaments. The distribution of local lineaments within studied area analyzed in terms of their orientation, length, frequency and intersection as well as the position, to show structural behavior of the studied area and later on to compare the result with fracture measuring from field. For analyzing local lineaments, firstly the studied area divided into 28 equal blocks, the area of each block approximately equal to $23km^2$ (Figure-17). Secondly; frequency and length rose diagram (Figure-18) as well as frequency, length and intersection contour maps for lineaments were constructed (Figure-19), in order to show the predominant direction and spatial distribution of local lineaments within studied area.

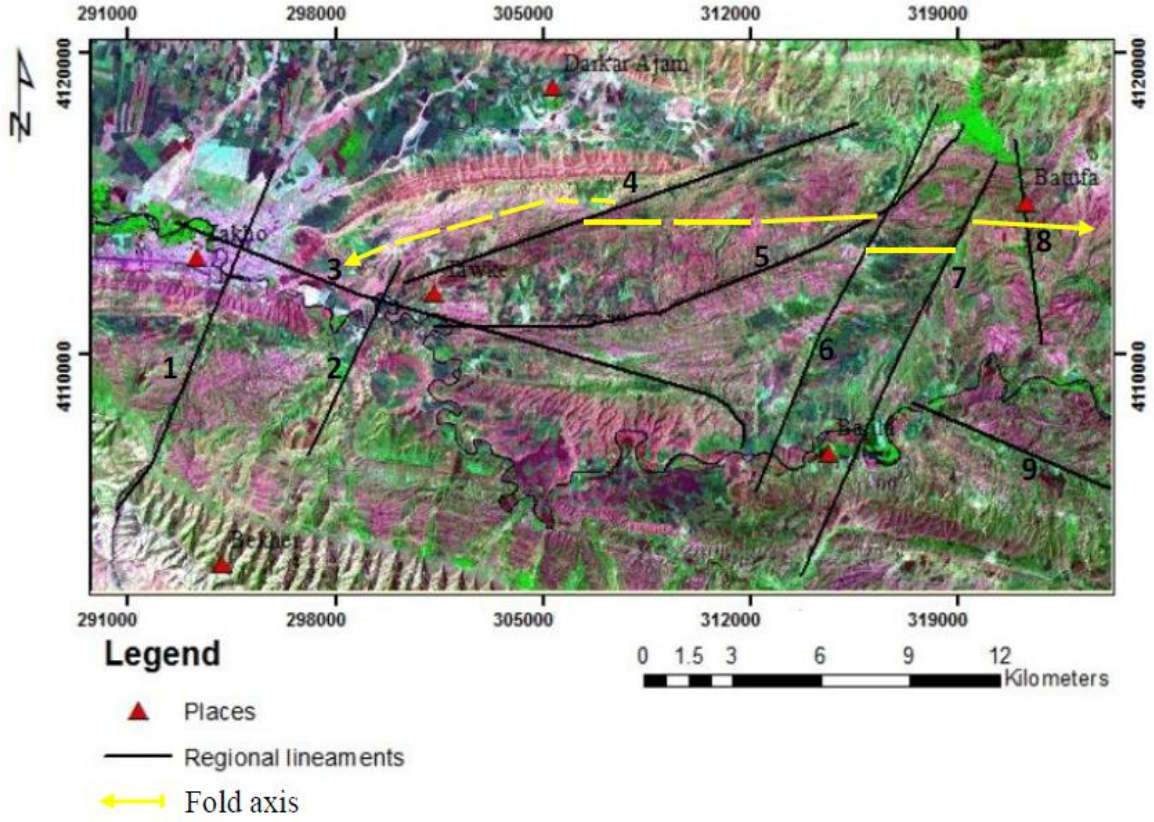

Figure-15: Regional Lineament map Taweke oil field and surrounding area.

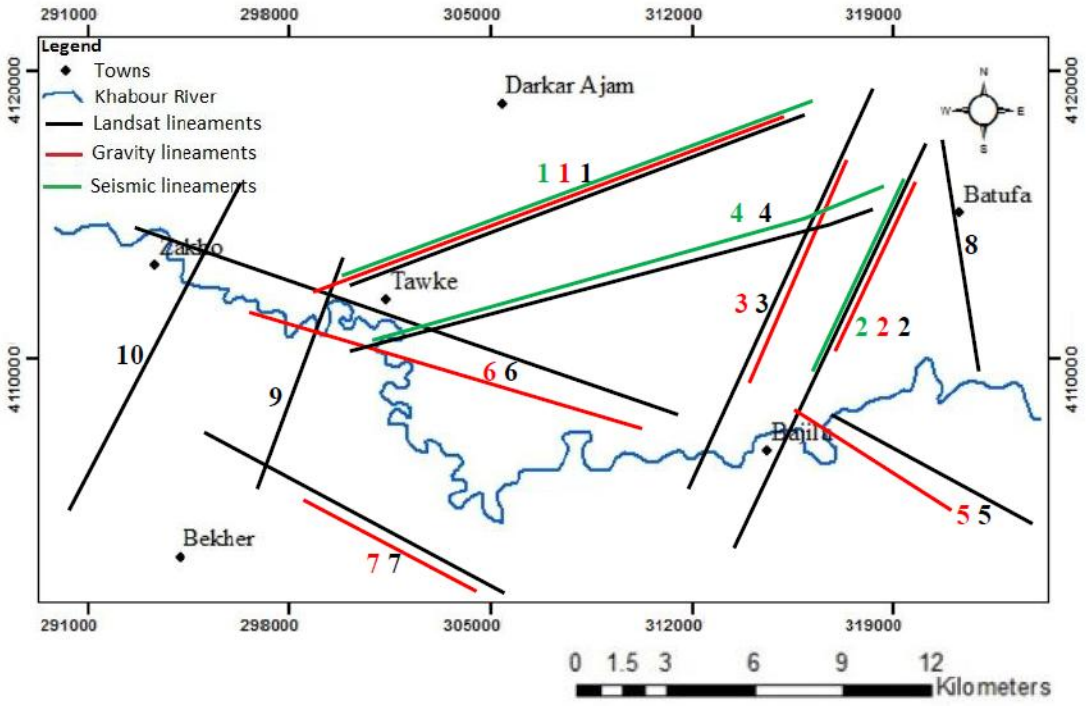

Figure-16: GIS integrated lineaments of both surface and subsurface in the studied area.

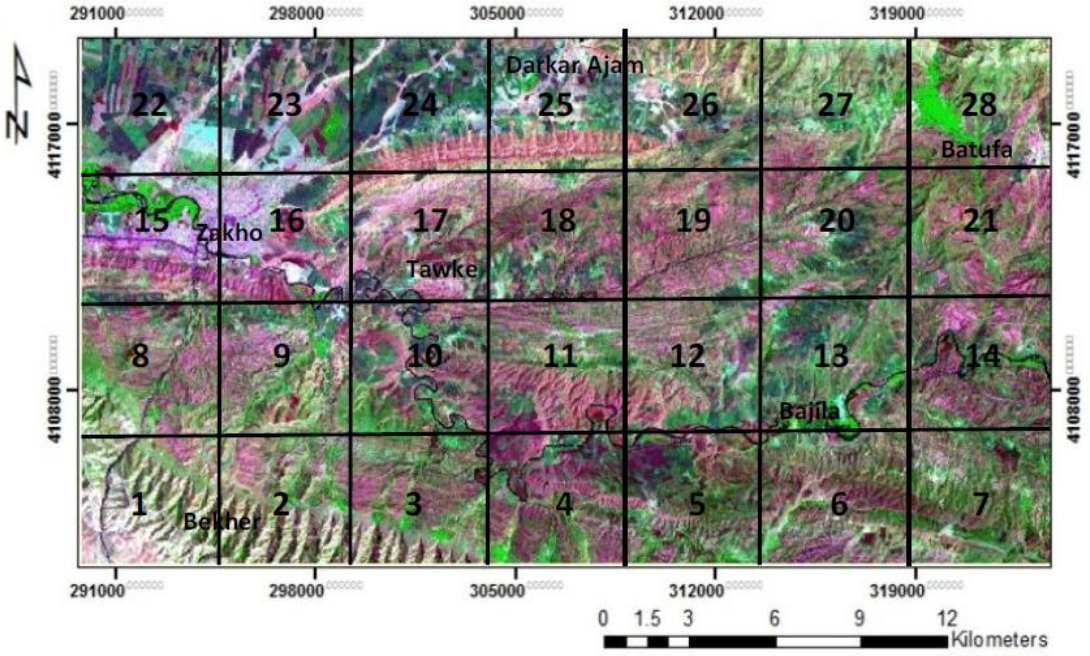

Figure-17: Map showing segmentation of studied area into blocks of equal area.

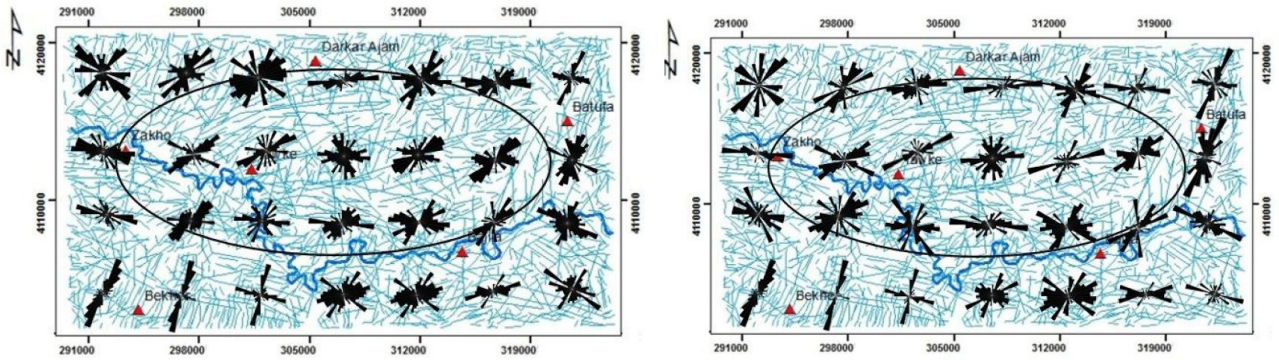

Figure-18: Frequency (a) and Length (b) Rose diagrams showing the orientation of lineaments within each block.

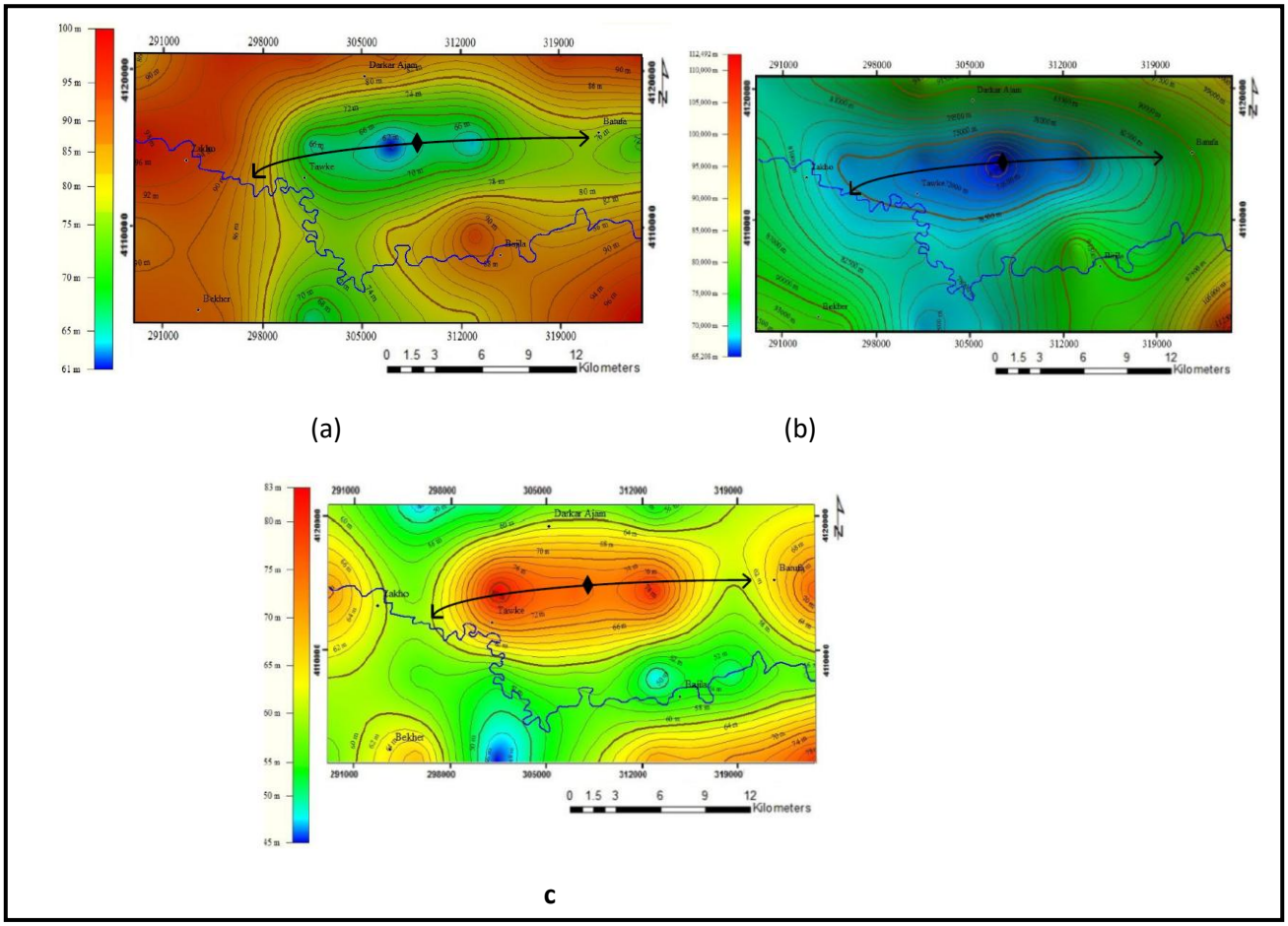

Figure-19:Frequency(a),Length(b)and intersection contour maps of Lineaments.

5.3.3. Ground truth and field observations

Field verification of the remotely sensed data is done in this study and for this purpose, ground truth was carried out to verify and correlate observed fracture such as joints, veins, fissures, and faults on the ground with local lineaments resulted from satellite images interpretation in position, directions and types of local lineaments . For that seventeen field stations were selected and scattered within different structural positions and geologic formations (Figure-20).Each station covered an area about 30X30 m and sometimes larger than that. The information which recorded in each station consist, attitude of bedding plane and fracture sets (joints, veins, fissures and faults), lithological compositions, and geological formation, fracture frequency as well as length of fractures were also measured. Geometrical classification of fractures was done with respect to fold axis using stereographic projection for each station.

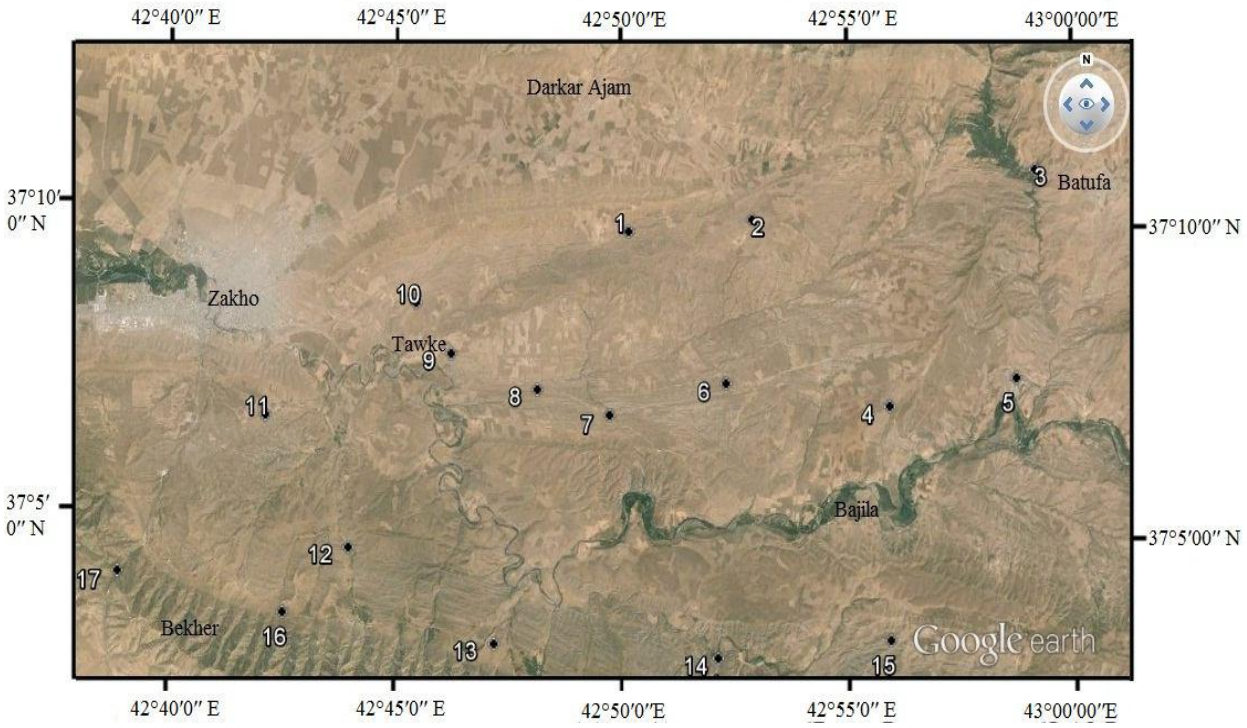

Figure-20: Satellite image from Google Earth showing field stations visited within studied area.

For fracture analysis a set of three orthogonal geometrical axes *a*, *b* and *c* ***[21]*** has been used to, describe the geometry of mesoscopic fractures. From fracture analysis (Table -5) two types of fractures were recognized; they are tension and shear fractures. Tension fractures represented as (ac) and (bc) fractures mostly appear in form of a sets, while shear fractures represented as systems or sets such as (hko, hol and okl). Paleostress analyzed either from some of the conjugate shear fractures systems or from single shear fracture sets depending upon rake angle of the striation on each fracture planes. The directions of principle stress axes are (355◦/14◦, 006◦/10◦) for (σ1), while (σ2) attitudes are (183◦/66◦, 192◦/70◦) and (σ3) attitudes are (085◦/17◦, 096◦/08◦) in stations(1 and 9). E-W stress direction with (σ1) attitudes (083◦/12◦, 268◦/16◦), (σ2) attitudes of (320◦/68◦, 088◦/70◦) and (σ3) attitude are (350◦/10◦, 180◦/12◦) fined in stations (4and 6). While extension stress analyzed from (hol) acute about (c) axis appears in station 17 that (σ1) has attitudes of (005◦/85◦), but a (σ2) attitude is (095◦/05◦), while a (σ3) attitude is (356◦/12◦). As well as the extension stress phase can be attained from station (8) when fracture system of (okl) acute about (c) analyzed for determination of paleostress whose (σ1) has attitude of (012◦/78◦) and (σ2) attitude is (210◦/20◦) while (σ3) attitude is (098◦/30◦). The two last fracture systems show that the (σ1) takes near to vertical direction which is a good indicator for vertical movement in the study area.

From above stress analysis three tectonic stresses were acted on this area, one is from north-south, second from East-West direction while the third stress form vertical direction to structure. The changing in orientation of the stress field especially N-Sand E-w direction attributed to variation of stress field due to stress relaxation during folding ***[22]***, while the vertical stress formed either due to vertical movement of basement faults, or neither due to uplifting of fold cause gravity collapsing within different parts of the fold.

Table -5: Stereographic projection and frequency rose diagrams for fractures measured in each station in the field.

Station No.	Sterographic projection for Fracture sets	Rose diagrams of strikes of fracture sets
1	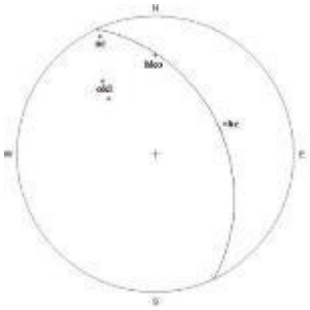	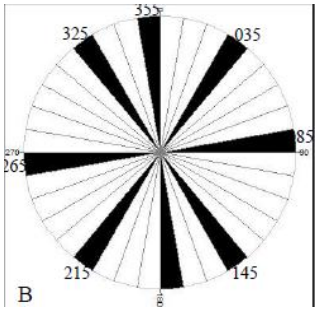
2	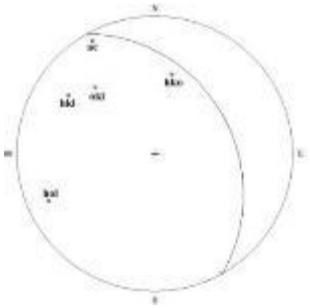	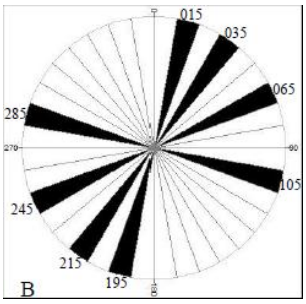
3	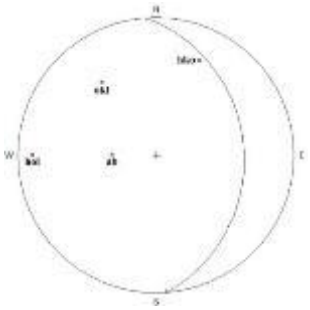	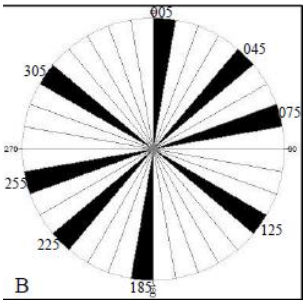
4	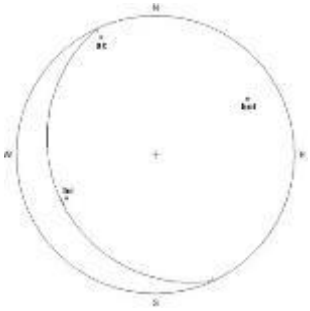	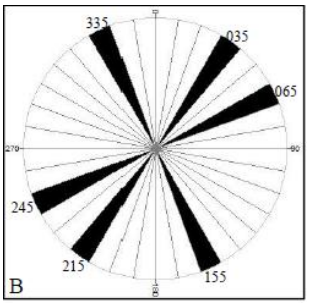

5	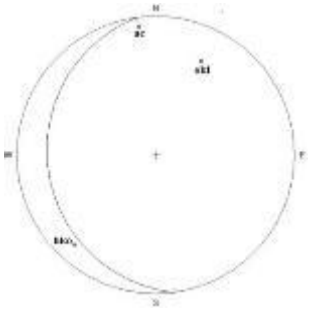	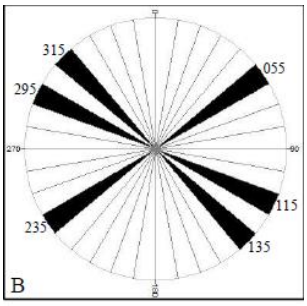 315 055 295 115 235 135 B
6	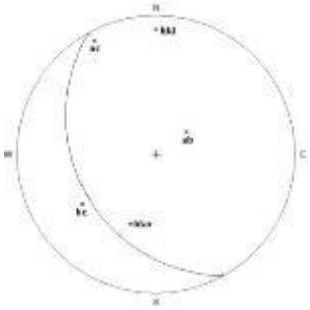	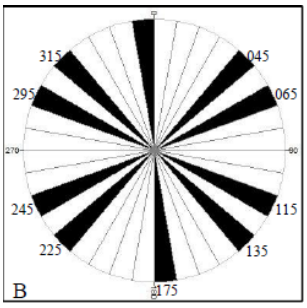 315 045 295 065 245 115 225 135 175 B
7	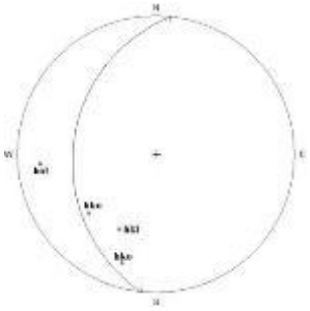	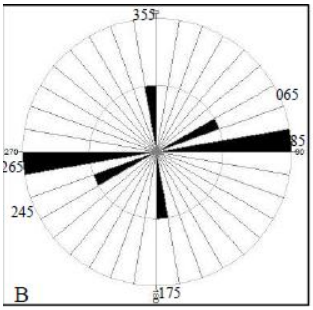 355 065 265 245 175 B
8	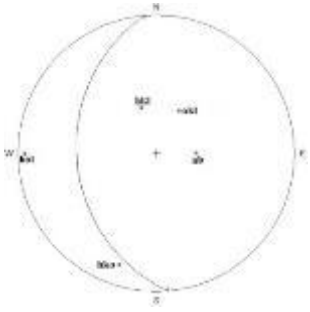	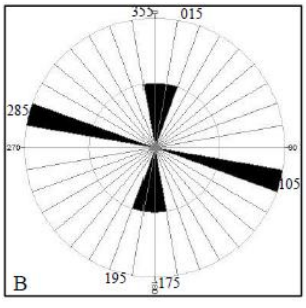 355 015 285 105 195 175 B

9	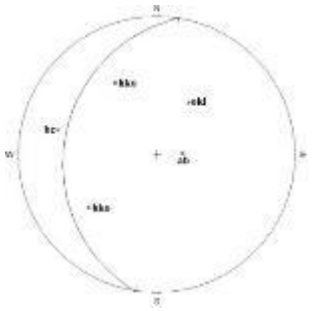	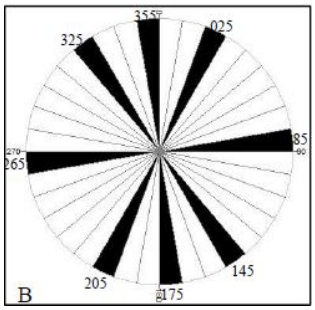 355 025 325 85 265 205 145 175 B
10	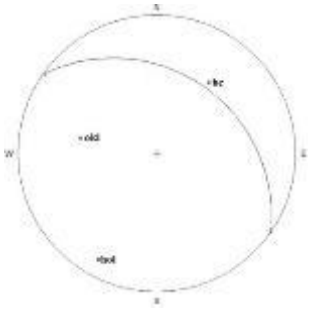	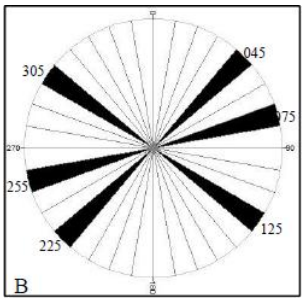 045 305 075 255 125 225 B
11	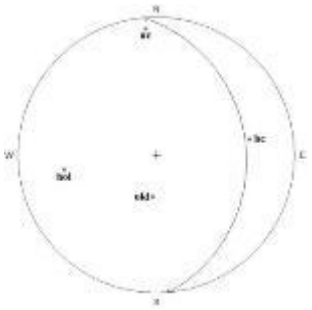	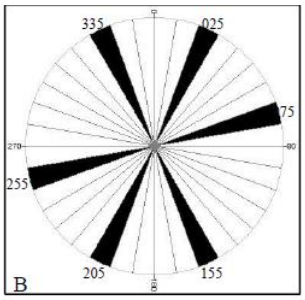 335 025 075 255 205 155 B
12	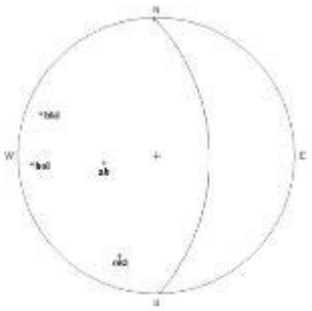	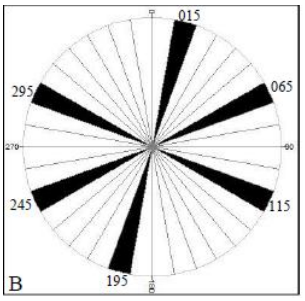 015 295 065 245 115 195 B
13	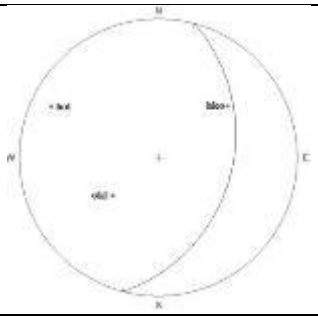	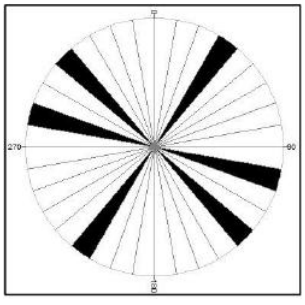

14	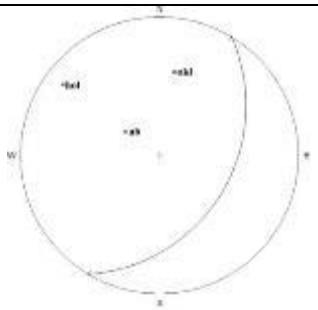	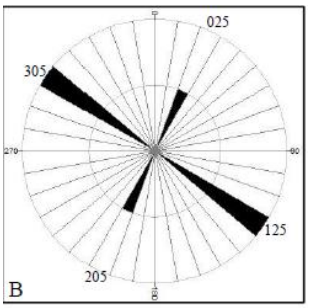 025 305 125 205 B
15	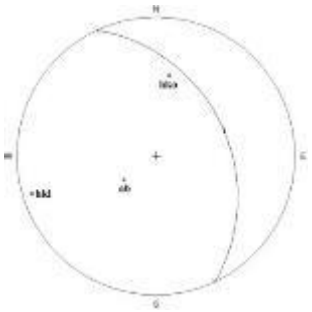	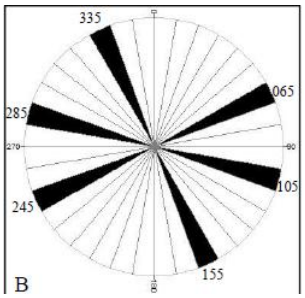 335 065 285 105 245 155 B
16	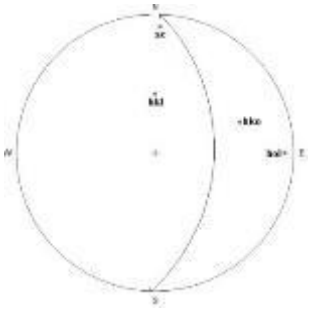	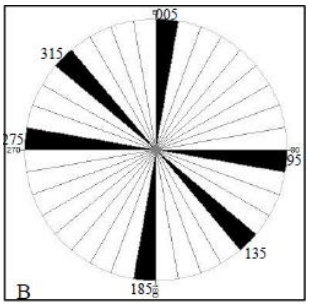 005 315 275 95 135 185 B
17	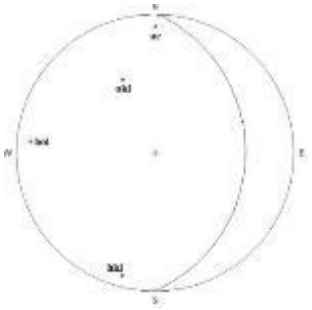	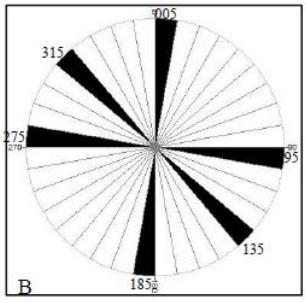 005 315 275 95 135 185 B

6. Tectonic discussion and conclusion:

6.1. Comparison of Local lineaments and Fracture analysis with referring to stress model:

6.1.1 .Local lineaments reflect fractures:

The comparison study of local lineaments indicate that there are very coherent relationship between local lineaments and fractures which appears in field stations, the coherency related to location, length, orientations and its position. Accordingly any distribution and conclusion related to mechanism and dynamic analysis of fractures has the same meaning when local lineament will analyzed. From analysis of fracture sets and systems, three successive main phases of stress conditions during the late stages of folding happened. In each phase several fracture sets are formed with a certain age. In the first main phase, fractures in (hol) acute about (a) system,(hko) acute about (a) system and ac-set are formed by primary compressive stresses from N-S direction perpendicular to fold axis , which are produced by the continental collision during Alpine orogeny between Arabian - anadolian plates. Fractures in (hol) acute about (a) system are formed when (σ1) becomes perpendicular to fold axis and parallel to bedding planes, whereas fractures belonging to (hko) acute about (a) system are formed when (σ2) becomes perpendicular to bedding planes and (σ3) parallel to fold axis. In the second main phase, fractures in (hko) acute about (b) system, (bc) set and (okl) acute about (b) system are formed by secondary stresses trending E-W parallel to fold axis, which are produced by an elastic rebound of primary compression***[23]*** . Fractures in (hko) acute about(b) system are formed when (σ2) becomes perpendicular to bedding planes and (σ3) perpendicular to fold axis, whereas fractures belonging to (okl) acute about (b) system are formed when (σ2) becomes perpendicular to fold axis and (σ3) perpendicular to bedding planes. During the last main phase, fractures in (hol) acute about (c) system, (bc) set, (okl) acute about (c) system and (ac) set are formed by vertical stresses, which are probably produced by the movements of basement blocks or due to gravity effect. Fractures in (hol) acute about (c) system are formed when (σ2) becomes parallel to fold axis and (σ3) perpendicular to fold axis, whereas fractures belonging to (okl) acute about (c) system are formed when (σ2) becomes perpendicular to fold axis and (σ3) is parallel to the fold axis. Usually, extension fractures are formed contemporaneously with shear fractures. However, most of the mesoscopic fracture sets and systems that are present in the studied area are geometrically related to bedding planes and in some localities related to fold axis of Tawake anticline. There is a good coincidence between the trends of local lineaments and mesoscopic fracture patterns in the studied area, which indicates that these lineaments are genetically related to Tawake anticline's evolution.

6.1.2. Graphical stress model for the Tawke structure, based on the directional analysis of local lineaments:

In structural geology, the notion of a graphical stress model is often used to illustrate the kinematic or mechanical aspects of a specific structural phenomenon seen as a discrete geological event. In this context, the stress model (Figure-21) basically represents a schematic figure showing the principal compressive stresses and types of local lineaments in relation to the axial trend of the anticline. The directions of the principal compressive stresses were inferred from the orientation of the anticlinal strike. The types of lineaments (i.e. shear and tension fracture traces) and their azimuthal ranges in the model were defined on the basis of rose diagram analysis and within the framework of the geometrical relationship between fold axis and local lineaments. The azimuthal tension regions (T) are N 0° - 15° E, N 0° -15°W, N 75° - 90° E and N 75° - 90° W. The azimuthal shear regions (S) are N 15 ° - 75° E and N 15 ° - 75° W. These are represented in the stress model of Tawke anticline (Figure-21).

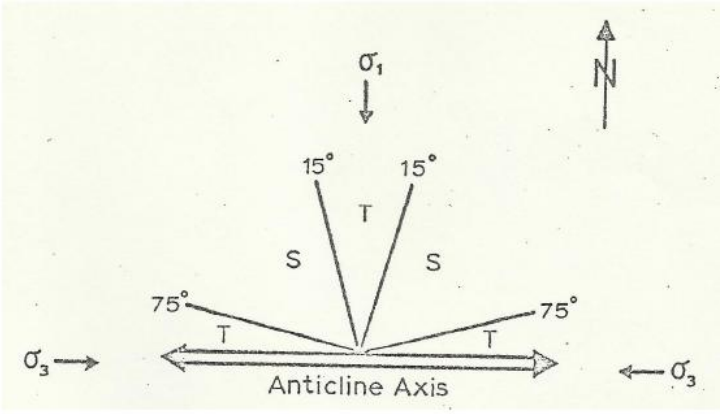

T.Tension fracture region.σ1.Maximum compressive stress.
S. Shear fracture region. σ3. Minimum compressive stress.

Figure-21: Graphical stress model in Tawke Anticline.

6.2. Comparison of Regional lineaments and geophysical data with tectonic implication:

The occurrence of the oblique and transversal with parallel regional lineaments along Tawake anticlinal structure represents significant features. The remarkable characteristic of these lineaments suggests that certain subsurface tectonic factors have caused or contributed to their occurrence. This assumption seems quite in agreement with a subsurface study carried out by ***[24,5].***The seismic sections and reflectors maps of upper cretaceous Formation show two reverse faults of NE direction with their up-throws away from each other. Both faults appear again on the subsurface seismic sections in the study area ***[5].*** The recurrence of these faults in several stratigraphic horizons at different depths and their great similarity in orientation, size and relative position to regional lineaments indicate a probable structural relationship between the faults and these lineaments. Other faults with different orientations can also be seen in the gravimetric lineaments particularly the fault which occurs in the east and southwest of the study area with NW-SE orientation. Although these faults as indicated by gravity and seismic lineaments coincide in size, orientation and positions with regional lineaments appears on satellite images, so these regional lineaments are manifestation of subsurface faults. These faults or lineaments forms at depth and growth up through sedimentary panel, and may be at a depth of basement, which seismic data not reach that depth, while gravity lineaments may reflect that.

6.3. General Tectonic Implication:

The present tectonic features of Middle East region have been ascribed to two major orogenies which occurred in the Middle – Late Cretaceous and late Tertiary, while the continuous vertical movements of basement blocks which surrounded by faults were recorded and have been occurring since the early to middle Paleozoic ***[25,26]*** .In the light of this tectonic history with structural observations recorded during this study, one cannot escape that both compressional forces and block-faulting were responsible for the structural architecture of the study area. In any attempt to explain the tectonic mechanism of the area, it would be very difficult to exclude one of these two tectonic events. The sediments which overlaid the unequally disturbed blocks prior to any particular orogenic movement must have formed a sheet of heterogeneous sediments. This must have been heterogeneous in the sense that neither its lithology nor the thickness of its sedimentary units should have been uniform across the whole area. The authors, therefore believe that the area as one which was initially covered with a heterogeneous sheet of sediments composed of an aggregate sedimentary sections (or segments) overlaying a block-faulted basement with very irregular

topography. Thus, the sedimentary sheet was lacking in both physical and lithological continuity and the homogeneity for transmitting stress. The regional compressive stress which was directed mainly from N-S, has affected the sedimentary sheet which filled and covered several small basins each of which has a different thickness of sediments, physical properties, and plane of decollement.

The regional stress also affected the fragmented basement and induced nudging and jostling of the blocks which produced unequally distributed and vertically directed secondary local stress fields. The sediment basin was independently folded primarily by the horizontal compression stress, and secondarily by vertically induced stress. The thicker sediments above detachment plane probably produced more pronounced fold, and larger basins produced larger folds. The lack of homogeneity of stress transmission and the deformation or sediments, has led to complex directional resolution of the stress fields in different parts of the area. This may well account for considerable differences in the axial orientations and alignments of the anticlines occurring within short distances, and also for certain structural aspects such as the asymmetry and axial plunging of some anticlines. It has been observed that compressive horizontal stress have been active since early as the Middle Cretaceous while the block-faulting dates from at least the Middle Paleozoic and continued intermittently up to Late Tertiary.

References

[1] Zwain, J. and Majeed, B.S. *Structural analysis of fracturing in Sinjar Anticline using remote sensing technique*, ACSM-ASPRS Annual convention Technical papers, Vol. 4, pp. 181- 190.(1988).

[2] Lee, M.K., T.C. Pharaoh and N.J. Soper, *Structural trends in central Britain from images of gravity and aeromagnetic fields*. J. Geol. Soc.London, 147: pp.241-258.(1990).

[3] Qari, M. Y. H. T., *Application of Landsat TM Data to Geological Studies, Al-Khabt Area, Southern Arabian Shield*. Photogrammetric Engineering and Remote Sensing. Vol. 57, No.4, pp. 421-429. (1991)

[4]Mohammed, A., Palanivel, K., and Kumanan, C.J., *Significance of Surface Lineaments for Gas and Oil Exploration in Part of Sabatayn Basin-Yemen.* Journal of Geography and Geology Vol. 2, No. 1. (2010).

[5] DNO, *Atlas of Tawke Field* .International Corporate Presentation, Erbil, Iraq. 46P. (2012)

[6] Bellen, R. C., Dunnington, H.V., Wetzel, R., and Morton, D. M., *Stratigraphic lexicon of Northern Iraq*. Gulf Petrolink, 03 10 asie (Iraq), 239p. (2005).

[7] AL-Musawi H.A., *The Geology of Zakho Quadrangle sheet NJ-38-9 scales1:250 000*, GEOSURV int.rep.no. 3110.Baghdad, Iraq.(2007)

[8]Sabins, F.F, *Remote Sensing: Principles and Interpretation*, (3rd Edn.), W.H. Freeman and Co. (1996).

[9] Babcock, E. A., and Sheldon, L.G., *Structural significance of lineaments visible on aerial photos of the Athabasca oil sands area near Fort Mackay, Alberta*, Bull. Of Canadian Petro. Geology, Vol. 24, No.3, pp.457-470. (1976)

[10] Gupat, R.P., *Remote sensing Geology*. Springer, Berlin, 656 pp. (2003)

[11] Lillesand, T. M. and R. W. Kiefer, *Remote Sensing and Image Interpretation*, Fourth Edition, John Wiley & Sons, NewYork, 724 p. (2000)

[12] Marcus Borengasser, William S. Hungate.p. cm. *Hyperspectral remote sensing : principles and applications*, Taylor & Francis Group, LLC, 119p. (2008)

[13] Suzen, M.L. and Toprak, V., *Filtering of Satellite Images in Geological Lineament Analyses: An Application to a Fault Zone in Central Turkey*, International Journal of Remote Sensing, 19(19), pp:1101-1114.(1998)

[14] Masoud, A. A. and Koike, K., *Auto-detection and integration of tectonically significant lineaments from SRTM DEM and remotely sensed geophysical data*, ISPRS Journal of Photogrammetry and Remote Sensing, Vol. 66, PP:818–832.(2011)

[15] Arlegui, L.E., Soriano, M.A. "*Characterizing lineaments from satellite images and field studies in the central Ebro basin (NE Spain)*", International Journal of Remote Sensing, Vol.19, No.16, pp:3169-3185.(1998)

[16] Rowan, L.C., and Mars, J.C. *Lithologic mapping in the Mountain Pass,California area using Advanced Spaceborne Thermal Emission and Reflection Radiometer (ASTER) data*, Remote Sensing of Environment, Vol. 84, pp. 350-366.(2003)

[17] Mc Carthy, J. S., Smith, M. J., and Hall, D. K. *Report on geological investigation of the area NE of Zakho site investigation* Co., England, NIMCO, Unpub. Report (264, 12), pp. 34-70. (1954)

[18]Buday, T., and Jassim, S.Z. *The Regional Geology of Iraq*,Vol.II:Tectonism, Magmatism, and Metamorphism. 352 p. (1987)

[19]Jassim, S. Z., and Goff, J, (eds.), *Regional Geology of Iraq*. Dolin, Prague and Moravian Museum, Brno, Czech Republic, 341p. (2006)

[20]Ramsey, I. A. P. *Relationship of fractures in unconsolidated superficial deposits to those in the underlying bed rock*. Modern Geology, 3, pp.25-41.(1971)

[21]Turner, F. J., and Weiss, L. E. *Structural Analysis of Metamorphic Tectonites*: New York, McGraw-Hill, 545 p. (1963)

[22]Van der Pluijm, B., and Marshak, S. *Earth Structure*, 2nd Ed., W. W. Norton & Company, pp.40-71, pp. 414-15. (2004)

[23]De Sitter, L.V.U. *Structural Geology*. McGrow-Hill, U.S.A. 551 P. (1964)

[24]AL-Dawoody A.N. M. *A Gravity Survey and Data Interpretation of Tawke Structure, Iraqi Kurdistan region.* Journal of Kirkuk University. 6,(3) ,(2011).

[25]Numan, N. M. S. *Major Cretaceous tectonic events in Iraq*. Ref. Jour. Sci.,11(3), pp. 32-52. (2000)

[26]Numan, N. M. S. *Cretaceous and Tertiary Alpine subductional history in northern Iraq*. Iraqi Jour. Earth Sci., 1 (2), pp. 59-74. (2001)